A CMOS Switched Transconductor Mixer

Eric A. M. Klumperink, *Member, IEEE*, Simon M. Louwsma, Gerard J. M. Wienk, and Bram Nauta, *Senior Member, IEEE*

***Abstract*—A new CMOS active mixer topology can operate at low supply voltages by the use of switches exclusively connected to the supply voltages. Such switches require less voltage headroom and avoid gate-oxide reliability problems. Mixing is achieved by exploiting two transconductors with cross-coupled outputs, which are alternatingly activated by the switches. For ideal switching, the operation is equivalent to a conventional active mixer. This paper analyzes the performance of the switched transconductor mixer, in comparison with the conventional mixer, demonstrating competitive performance at a lower supply voltage. Moreover, the new mixer has a fundamental noise benefit, as noise produced by the switch-transistors and LO-port is common mode noise, which is rejected at the differential output. An experimental prototype with 12-dB conversion gain was designed and realized in standard 0.18-μm CMOS to operate at only a 1-V supply. Experimental results show satisfactory mixer performance up to 4 GHz and confirm the fundamental noise benefit.**

***Index Terms*—Active circuits, active mixers, CMOS analog integrated circuits, communication circuits, demodulation, dielectric breakdown, down-conversion mixers, frequency conversion, integrated circuit noise, intermodulation distortion, linear transconductance, low-noise design, low-voltage, microwave integrated circuits, microwave mixers, modulation, noise, nonlinear circuits, receiver, reliability, transmitter, white noise, $1/f$ noise.**

I. Introduction

MIXERS are commonly used for frequency translation in radio frequency (RF) communication systems. The frequency translation results from multiplication of the RF input signal with a "local oscillator" (LO) signal. In practice, mixers are preferably implemented using "hard switching" via a large LO signal, which mathematically corresponds to multiplication with a square wave, instead of a sine wave. This renders 2 dB higher conversion gain ($2/\pi$ instead of 1/2) and lower noise figure [1].

A key problem for the realization of analog circuits in current and future digital CMOS technology is the continuously reducing supply voltage for each technology generation, resulting in nonconducting or poorly conducting switches conveying voltages in the "middle voltage range" between the supply voltages [2]. This is a severe problem in analog and mixed analog–digital circuits exploiting switches, like A/D and D/A converters and switched capacitor circuits, but also in mixers. This paper deals with a "switched transconductor" mixer topology [3], aiming for low-voltage operation by exploiting exclusively switches connected to the supply voltages. Assuming ideal switching, it realizes a transfer function equivalent to a conventional active mixer. The current paper analyzes the mixer performance in detail and compares it to a conventional active mixer. Competitive performance is found, while operating at a much lower supply voltage.

Manuscript received December 10, 2003; revised February 23, 2004.

The authors are with MESA+ Research Institute, University of Twente, 7500 AE Enschede, The Netherlands (e-mail: e.a.m.klumperink@utwente.nl).

Digital Object Identifier 10.1109/JSSC.2004.831797

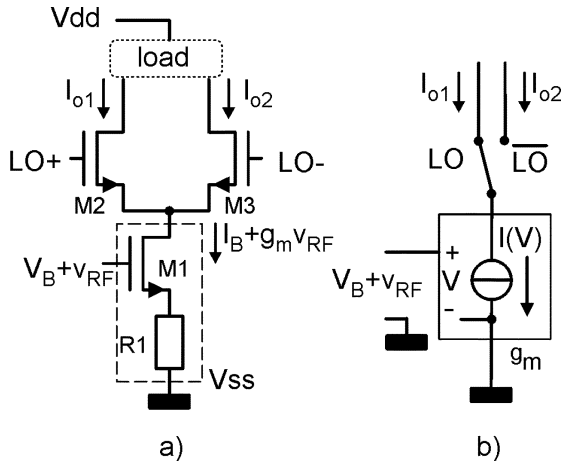

Fig. 1. (a) Single balanced active MOS mixer. (b) Functional representation for large switching signals.

The contents of this paper are as follows. First, we will discuss this mixer-switch problem in Section II, taking a commonly used active CMOS mixer as a starting point. The "switched transconductor" mixer will then be proposed in Section III. Section IV analyzes its performance in more detail, comparing to a conventional active mixer. In Section V, simulation results are presented to verify the results of the theoretical analysis. Experimental results on a 1-V switched transconductor mixer realized in 0.18-μm CMOS are reported in Section VI, while the conclusion is presented in Section VII.

II. Switch Problem in Conventional Mixers

Active mixers are commonly used in RF CMOS transceiver circuits [1]. Fig. 1(a) shows a single balanced version of a simple active mixer configuration. It consists of a transconductance stage $(\mathrm{M1}+\mathrm{R1})$, switches (M2 and M3), and a load network. Voltage V_{B} biases the transconductance stage at a current I_B and transconductance g_m, resulting in a voltage-to-current conversion from v_{RF} to drain–current variation $g_m v_{\mathrm{RF}}$. Source degeneration resistor R1 may be added for wide-band linearization. The switches M2 and M3 are driven by anti-phase LO signals, denoted here as $\mathrm{LO}+$ and $\mathrm{LO}-$. To mimic multiplication with a square wave with frequency f_{LO}, the LO amplitude must be chosen sufficiently high to fully switch the transconductor current $I_B + g_m v_{\mathrm{RF}}$ to either I_{o1} or I_{o2}. For the purpose of a first-order functional analysis, we can model the operation of M2 and M3 as switches driven by the logic signal LO and its inverse $\overline{\mathrm{LO}}$, as shown in Fig. 1(b). Actually, M2 and M3 are preferably operated in saturation, to act alternatingly as cascode devices for M1, improving output resistance

and linearity. Transistor M1 with resistor R1 can be modeled as a voltage-controlled current source with large-signal $I(V)$ function, realizing a small-signal transconductance g_m defined by the value of input bias voltage V_B.

Depending on the application, output currents I_{o1} and I_{o2} are connected to different load networks. For example, resistors to the positive supply voltage $V_{\rm dd}$ may be used, to provide broadband voltage conversion gain, or tuned LC networks for narrowband gain. As we want to focus on the V–I core that realizes the frequency translation, we will omit this load network for now. Thus, the mixer has a conversion transconductance, instead of conversion voltage gain.

Consider now the operation of this circuit for low supply voltages. To achieve conversion gain, good linearity, and low noise, transistor M1 in the g_m stage is usually biased well in strong inversion and saturation. Resistive degeneration for wideband linearization also requires voltage headroom. Moreover, to reduce nonlinearity degradation due to the nonlinearity of the drain–source conductance, a drain–source voltage well above the saturation voltage is needed [4], [5]. Simulations and measurements indicate that more than $V_{\rm DS} > 0.5$ V is required for M1, to achieve an IIP3 well above 0 dBm (in 50 Ω) at 10-dB conversion gain in an 0.18-μm process. With threshold voltages around 0.5 V, this means that the *minimum* voltage at the gate of M2 and M3, to switch these devices on, is typically higher than 1 V. For low $V_{\rm dd}$ voltages on the order of 1 V, extra switch driver circuits are therefore required to drive the gate well above $V_{\rm dd}$. Due to gate-oxide tunneling and reliability issues, this is only acceptable to some extent [7]. With decreasing oxide thickness, this problem is likely to become more serious in future CMOS processes [8].

Even if oxide reliability is no issue, the conventional method of operating the switch transistors M2 and M3 in saturation requires significant voltage headroom, reducing the headroom available for the load and hence limiting the achievable conversion gain. Different solution have been proposed for this problem with various pros and cons. For instance, if the bandwidth is limited, transformer coupling to transfer the transconductor current to the switches can save voltage headroom [6], however, at the cost of large chip area. Active mixers with a folded topology have also been proposed, e.g., with PMOS switches following an NMOS transconductance stage [9]. However, this requires adding a bias current source that adds substantial noise, unless significant voltage headroom is reserved (but then the switch again becomes the problem).

In the next section, we propose a mixer requiring almost no voltage headroom across the switch that works with gate voltages within the supply range, so that oxide reliability also is guaranteed.

III. Switched Transconductor Mixer

The key to the new mixer is to *avoid* requiring a conductive channel at a voltage level in "the middle range" between the supplies $V_{\rm ss}$ and $V_{\rm dd}$. Note that it is easily possible to make a low ohmic switch without oxide reliability issues, provided that its conductive channel is connected to either $V_{\rm ss}$ (NMOST) or $V_{\rm dd}$ (PMOST). We can rely on this in future CMOS technologies, for the simple reason that digital logic circuits rely on this functionality (e.g., in inverters). Moreover, low ohmic switches reduce switch voltage headroom to almost zero.

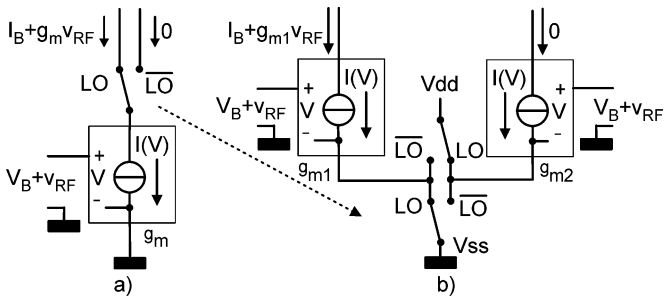

Fig. 2. (a) Conventional mixer. (b) Switched transconductor mixer concept: two transconductors g_{m1} and g_{m2} are activated alternately by the switches, implementing the same function.

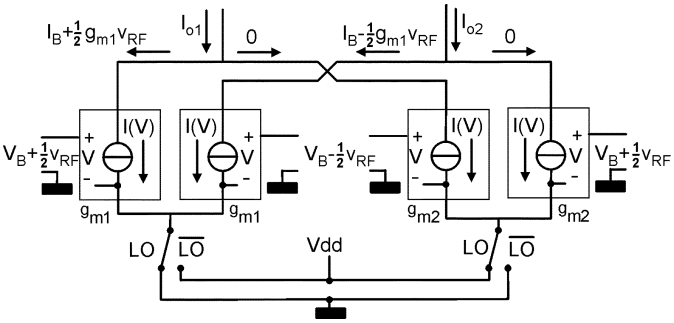

Fig. 3. Double-balanced switched transconductor mixer.

Fig. 2(a) shows the conventional active mixer and Fig. 2(b) shows how the same functionality can be achieved using *two matched transconductors* g_{m1} and g_{m2} and *switches connected to voltages* $V_{\rm ss}$ *and* $V_{\rm dd}$ *only*. The transconductors have a nonlinear $I(V)$ characteristic, with transconductance g_m around bias point (V_B, I_B). Each transconductor is either switched on to this bias point (V_B, I_B) by a switch to $V_{\rm ss}$ or switched off by a switch to $V_{\rm dd}$. Thus, effectively, transconductance g_{m1} is on, if g_{m2} is off, and the other way around. Now, for matched transconductors and ideal instantaneous switching, either I_{o1} or I_{o2} is equal to $I_B + g_m v_{\rm RF}$, and the other current is zero, just as in the conventional mixer in Fig. 2(a). Thus, the circuits implement the same mixer function in different ways: the conventional mixer by a transconductor followed by current switching, and the new mixer by *switched transconductors*.

Single-balanced mixers have a strong output signal at the LO frequency, which can be canceled in a double-balanced version. By adding two additional transconductors driven by an antiphase RF signal, as shown in Fig. 3, this is readily implemented. Just as for the conventional active mixer, the double-balanced version has the same conversion gain as the single balanced version, because the RF voltage is divided over two transconductors (see Fig. 3).

IV. Relative Performance Analysis

We will now analyze the performance of the switched transconductor mixer in more detail, focusing on a comparison with the conventional double-balanced active mixer, which is functionally equivalent. For briefness, we will sometimes refer to the conventional mixer as "Gm + Sw" and to the switched transconductor mixer as "SwGm." The analysis procedure is analogous to the one in [10].

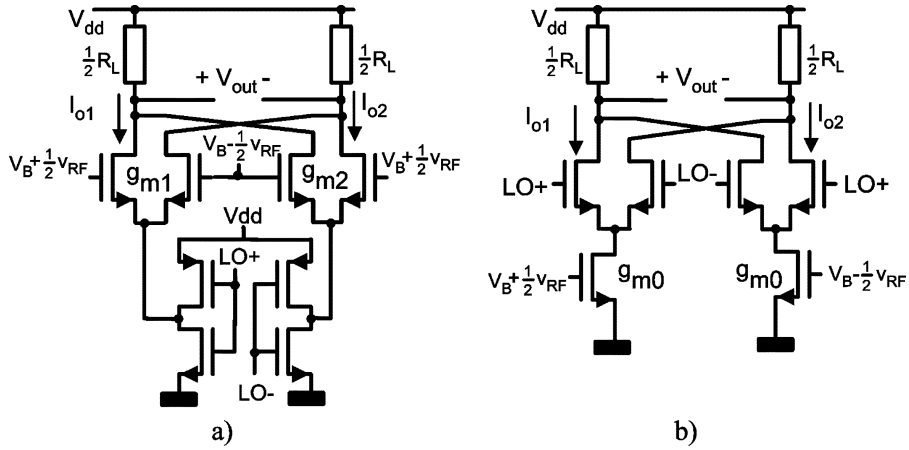

Fig. 4. (a) Double-balanced switched transconductor (SwGm) mixer with NMOS-transconductors and CMOS inverters as switches. (b) Conventional double-balanced active mixer Gm+Sw, also with NMOS transconductors.

A. Conversion Gain

Fig. 4(a) shows a double-balanced SwGm mixer, with two NMOS differential pairs acting as transconductor g_{m1} and g_{m2}, and two antiphase-driven CMOS inverters implementing the LO switches. Consider first the left half of the mixer, with transconductor g_{m1}. If the switches have a sufficiently low ON-resistance, the differential transconductor can be subdivided in two independent transistors, each acting as a transconductor. If capacitive effects are ignored, the output current $I_{o1,gm1}$ is a function of the instantaneous LO voltage $V_{\rm LO}(t)$ and the RF input voltage $V_B+1/2v_{RF}$, where V_B is the dc bias voltage of the RF input and $v_{\rm RF}$ is the small-signal RF-input voltage as follows:

$$I_{o1,gm1} = F\left(V_{\rm LO}(t), V_B + \frac{1}{2}v_{\rm RF}\right). \tag{1}$$

Since $v_{\rm RF}$ is small, a first-order Taylor expansion can be used as an approximation:

$$I_{o1,gm1} \cong F\left(\mathrm{V_{LO}(t)}, \mathrm{V_B}\right) + \frac{\partial F\left(\mathrm{V_{LO}(t)}, \mathrm{V_B}\right)}{\partial \mathrm{V_B}} \cdot \frac{1}{2}v_{\rm RF} \tag{2}$$

which can be rewritten as

$$I_{o1,gm1} = I_{B1}(t) + g_{m1}(t) \cdot \frac{1}{2}v_{\rm RF} \tag{3}$$

where $I_{B1}(t)$ is the time-variant bias current of transconductor g_{m1}, and $g_{m1}(t)$ is its time-variant transconductance of the individual transistors, resulting in mixer operation. The same analysis for the antiphase RF signal path via g_{m1} to I_{o2} renders

$$I_{o2,gm1} = I_{B1}(t) - g_{m1}(t) \cdot \frac{1}{2}v_{\rm RF}. \tag{4}$$

Subtraction renders the differential output current $I_{o,gm1}$ as follows:

$$I_{o,gm1} = I_{o1,gm1} - I_{o2,gm1} = g_{m1}(t) \cdot v_{\rm RF}. \tag{5}$$

Note that the I_B cancels in this differential output and that $g_{m1}(t)$ determines the conversion transconductance. For ideal instantaneous switching, a square-wave transconductance function with period $T_{\rm LO}$ results, switching between zero and an "ON-value" of g_{m0}. The value of g_{m0} is primarily determined by the $I(V)$ characteristic of the g_{m1} devices and the bias voltage V_B. If the switches have nonnegligible series resistance compared to $1/g_{m0}$, the conversion transconductance is somewhat lower (a detailed analysis will follow in Section IV-D).

In order to find the contribution of g_{m2}, a similar derivation gives

$$I_{o,gm2} = g_{m2}(t) \cdot v_{\rm RF} \tag{6}$$

where g_{m2} is activated by the inverse of the LO signal. In the case of 50% duty cycle, we have

$$g_{m2}(t) = g_{m1}\left(t + \frac{T_{\rm LO}}{2}\right). \tag{7}$$

The overall differential output current thus becomes

$$I_o = I_{o,gm1} - I_{o,gm2} = (g_{m1}(t) - g_{m2}(t)) \cdot v_{\rm RF} = g_{\rm eff}(t) \cdot v_{\rm RF}. \tag{8}$$

In many cases, we want to convert the differential current to a differential output voltage, using two load resistors. If the resistors have a value of $R_L/2$, the output voltage is

$$V_{\rm out} = -\frac{R_L}{2}(I_{o,gm1} - I_{o,gm2}) = -g_{\rm eff}(t) \cdot \frac{R_L}{2} \cdot v_{\rm RF}. \tag{9}$$

The ON- and OFF-switching of the transconductance takes time, resulting in reduced conversion gain at high-frequency LO frequencies. A piecewise linear approximation of $g_{m1}(t)$ and $g_{m2}(t)$ by a trapezoid function is instrumental to gain insight into the behavior of the mixer. Fig. 5 shows an example of the key time-variant variables, for the practical case that the transconductance time function is a trapezoid function, with equal ON- and OFF-switching times $\tau_{\rm sw}$. Although equality of the ON- and OFF-switching times is not critical, large differences in the switch times lead to reduced conversion gain and larger variations in the common-mode output bias current $(I_{B1}(t) + I_{B2}(t))/2$. Moreover, assuming equal ON- and OFF-switching

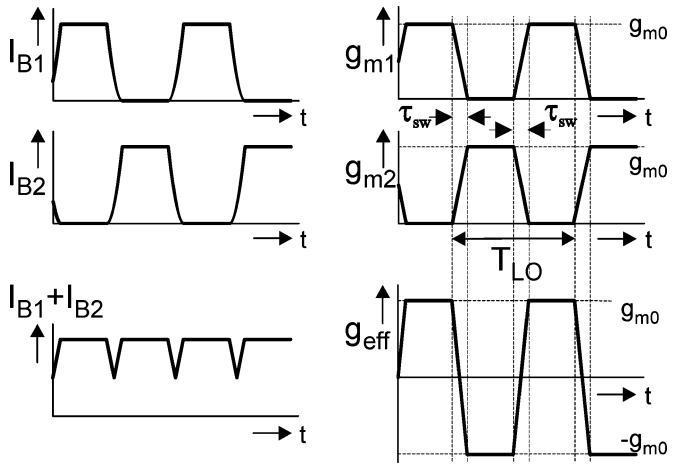

Fig. 5. Waveforms occurring in the switched transconductor mixer for the case with equal ON- and OFF-switching times $\tau_{\rm sw}$ for the transconductors.

times is convenient for a direct comparison with a conventional active mixer as analyzed in [10], where a trapezoid-like conversion transconductance is also used to model mixer operation for large LO voltage amplitude, with finite dV/dt around the zero-crossing of the LO voltage.

Taking finite switch-time into account, as in [10], a first-order approximation of the conversion gain CG of the SwGm mixer, terminated with a differential load resistance R_L, becomes

$$CG \approx \frac{2}{\pi}\left(\frac{\sin(\pi \cdot f_{\rm LO}\tau_{sw})}{\pi \cdot f_{\rm LO}\tau_{\rm sw}}\right) \cdot g_{m0} \cdot \frac{R_L}{2}. \qquad (10)$$

For low LO frequencies, the CG is equal to the familiar $2/\pi$ times $g_{m0}R_L/2$, corresponding to mixing with a square wave. Furthermore, only odd-order harmonics of the LO are produced at the output. It can be shown that this also remains true in case of unequal ON- and OFF-switching times for the transconductor, as long as the g_{m1} and g_{m2} waveforms remain equal and are time-shifted by $T_{\rm LO}/2$. Thus, assuming a trapezoid time function for $g_{m,\rm eff}$, *the same conversion gain as for a conventional mixer is found*.

Note, however, that the mixer functionality is implemented in a different way. In the conventional mixer, the V–I conversion is time-invariant, while the resulting currents are multiplied by $+1$ and -1. In contrast, the switched transconductor mixer exploits *time-variant* V–I conversions: both $g_{m1}(t)$ and $g_{m2}(t)$ are such that they alternately multiply by g_{m0} and 0, but time-shifted by $T_{\rm LO}/2$. While the signal transfer is equal to that of a conventional active mixer, this is not the case for the noise and nonlinearity, as will be shown in the next subsections.

B. Thermal Noise

The transconductance devices not only produce the useful output signal, but simultaneously also inject thermal noise, which can be modeled as a drain current with a variance equal to $4kT\gamma g_m \Delta f$. Analysis shows that this noise contribution is roughly the same for a SwGm and Gm+Sw at equal conversion transconductance. This makes sense, as either g_{m1} or g_{m2} is active, alternately producing (uncorrelated) thermal noise with a variance proportional to g_{m0}. However, there is a significant difference if we consider the noise contribution of the switch devices. In the double-balanced switched transconductor mixer in Fig. 4(a), the noise current introduced by the switching devices results in a common-mode output noise current. Thus, this noise current *cancels* in the *differential* voltage output. For the conventional double-balanced mixer in Fig. 4(b), the situation is completely different. This is because there is a *direct noise current path* between the outputs terminals during a time interval around the zero-crossing of the LO voltage. If the nodes LO+ and LO- have approximately the same voltage, both switch transistors conduct and have significant noise current, resulting in a noise peak around the zero-crossing [10], contributing noise at the IF frequency. Also, the noise due to gate resistance of the switch transistors is amplified during this time interval [1], [10]. This noise comes on top of the noise of the transconductance stage and tends to dominate at high LO frequencies. A similar effect occurs in passive mixers. For the conventional active mixer in Fig. 4(b), an approximation for the single sideband noise figure has been derived as [10]

$$\mathrm{NF}_{\rm SSB,Gm+Sw} = \frac{\alpha}{c^2} + \frac{2(\gamma_{\rm Gm} + r_{g,\rm Gm}g_{m0})g_{m0}\alpha + 4\gamma_{\rm Sw}\overline{G_{\rm Sw}} + 4r_{g,\rm Sw}\overline{G_{\rm Sw}^2} + \frac{1}{R_L}}{c^2 g_{m0}^2 R_s} \qquad (11)$$

where the transconductance, noise excess factor and gate resistance of the gm-driver stage are denoted by g_{m0}, $\gamma_{\rm Gm}$, and $r_{g,\rm Gm}$, respectively, while the corresponding properties are the switching stage are denoted by $G_{\rm Sw}$, $\gamma_{\rm Sw}$, and $r_{g,\rm Sw}$ and the bar refers to time averaging [10]. Resistor R_s is the resistance of the signal source used for noise figure evaluation (usually 50 Ω). Parameter α models the effective noise folding ($= 1$ for low LO frequency) and is equal to the power of the waveform $p_1(t)$ (equivalent for $g_{\rm eff}(t)$), which, in the case of a trapezoid approximation, can be approximated by [10]

$$\alpha \cong 1 - \frac{4}{3}\tau_{\rm sw} f_{\rm LO}. \qquad (12)$$

Using the same symbols, an analysis analogous to [10] for the switched transconductor mixer results in

$$\mathrm{NF}_{\rm SSB,SwGm} = \frac{\alpha}{c^2} + \frac{2(\gamma_{\rm Gm} + r_{g,\rm Gm}g_{m0})g_{m0}\alpha + \frac{1}{R_L}}{c^2 g_{m0}^2 R_s}. \qquad (13)$$

Comparing the equations, it appears that the expressions are identical, except that terms with $G_{\rm Sw}$ are lacking. This reflects the fact that noise from the switch transistors and LO port results in a common-mode output current, which is rejected if the differential output is taken. The rejection is perfect if the g_m-pair has zero differential voltage. However, simulations shows that, even when the differential transconductor pair is driven to its 1-dB compression point, considerable reduction is found and noise due to the switches becomes negligible. Thus, we conclude that the switched transconductor has a fundamental advantage in thermal noise, as the noise of the switch devices is negligible.

TABLE I
OVERVIEW OF THE MAIN PROPERTIES OF THE PROPOSED SWITCHED TRANSCONDUCTOR (SWGM) AND CONVENTIONAL ACTIVE MIXER (GM+SW)

Property	SwGm	Gm+Sw
Maximum Conversion Gain	$g_{m0} \cdot 2/\pi$	$g_{m0} \cdot 2/\pi$
Peak LO-voltage	$V_{GS,SWITCH}$	$V_{DS,Gm}+V_{GS,SWITCH}$
Thermal noise of gm	$\propto g_{m0}$	$\propto g_{m0}$
1/f noise of gm	Only partly mixed up	Mixed up
Noise of switch devices	common mode (rejected)	differential noise

C. Flicker Noise

In the conventional active mixer, $1/f$ noise of the transconductors is up-converted by the multiplying alternatingly by $+1$ and -1. Due to mismatch in the switches, low-frequency noise does exist at the output of the mixer via the two mechanisms outlined in [11].

In the switched bias mixer, the noise of the transconductors is only partially up-converted. If we model the $1/f$ noise as a time-invariant equivalent input noise voltage source in series with the gate,[1] this noise voltage is alternately multiplied by 0 and g_{m0}, by each transconductor. For an ideal square wave, the analysis is easy: due to the dc term of 1/2 in the Fourier series of the square wave, half of the $1/f$ noise power "remains" in the baseband, while the other half is mixed up around harmonics. Also, the output noise is alternatingly produced by g_{m1} and g_{m2}, which have uncorrelated $1/f$ noise. Overall, this leads to only 3 dB less $1/f$ noise than for a constant biased MOSFET pair biased at V_B. Thus, the switched transconductor mixer shows significantly more $1/f$ noise due to the transconductance devices then does a conventional active mixer. Resistive degeneration of the transconductor transistor helps to reduce this effect.

In the conventional active mixer, the switch devices can also contribute significant $1/f$ noise, especially at high LO frequencies [11]. In contrast, the switched transconductor has negligible $1/f$ noise of the switch devices (common-mode noise is rejected).

D. Switch Resistance and Linearity

As mentioned in Section IV-A, the finite ON-resistance of the switches may reduce the conversion gain. In order to estimate this effect, we can model the switch with a resistance $R_{\mathrm{sw,on}}$. The main effect of $R_{\mathrm{sw,on}}$ is a voltage drop, reducing the gate–source overdrive voltage of the transconductance transistors and, hence, g_m. As the ON-resistance of the switch decreases with LO amplitude, conversion gain increases with LO amplitude. However, using sufficiently wide switches, the effect becomes weak. Apart from this effect, switch resistance also "allows" for source voltage variation, due to the common-mode current of the two MOSFETs that constitute a differential transconductor. This voltage can mix with the RF voltage at the gate via the second-order term of the MOSFET, resulting in a differential output current of

$$i_{\mathrm{out}} = g_1 v_{\mathrm{RF}} + \left(\frac{g_3}{4} - \frac{g_2^2 R_{\mathrm{sw,on}}}{1 + 2 g_1 R_{\mathrm{sw,on}}} \right) \cdot v_{\mathrm{RF}}^3 \qquad (14)$$

where g_1, g_2, and g_3 are the taylor series coefficients derived by taking the derivative of $I_d(V_{\mathrm{gs}})$ of the transconductor MOSFET. As g_3 is negative [12], while g_2 is positive for a saturated MOSFET in strong inversion, the additional g_2 term will lead to increased third-order distortion.[2] However, if the switch resistance is significantly lower then $1/g_1$, the linearity penalty can be small, as will be shown in the next section.

V. SIMULATION RESULTS

In order to verify the analysis from the previous section, the switched transconductor mixer (SwGm) and conventional active mixer (Gm+Sw) have been compared using Spectre periodic steady-state (PSS) simulations and MOS Model 9 models for an industrial 0.18-μCMOS process. Table I gives a summary of the expected differences as analyzed in Section IV. Table II lists the design parameter values used during simulations. We will first discuss the motivation for these parameter choices and then discuss the simulation results.

Whenever possible, parameters were chosen to be equal for both mixers. However, we chose to use a 1.5-V supply for the conventional mixer to allow for "conventional" operation in strong inversion and saturation for all MOSFETs (otherwise conversion gain, linearity, and noise are degraded by triode operation). In contrast, the switched transconductor operates at a 1-V supply, with approximately a 40-mV voltage drop across the switch devices, operating in triode. In both mixers, the transconductors were somewhat arbitrarily implemented using 15/0.36 N-MOSFETs, nominally biased at $V_{\mathrm{GS}} = V_{\mathrm{DS}} = 0.6$ V (0.5 V threshold voltage), aiming for a conversion transconductance on the order of 1 mS.

For both mixers, two CMOS inverters were used as LO buffers to drive the switches, as is typically required to reduce the loading of the local oscillator and avoid effects like LO pulling. All LO buffers operate at $V_{\mathrm{dd}} = 1$ V and are driven by balanced sinewave signals with 0.5 V amplitude, around a common-mode voltage of 0.5 V. In both mixers, switch sizes were chosen for equal input capacitance, resulting in very similar trapezium-like waveforms at the output of the LO buffers, with 1 $V_{\mathrm{pk-pk}}$. The LO signals are AC coupled to the LO inputs of the mixers, via high-pass networks with negligible attenuation. AC coupling is actually not necessary for the switched transconductor, but is convenient for the conventional mixer to define the common-mode LO voltage, which was chosen equal to 1 V, to keep the transconductance stage in saturation. The next subsection motivates the choice of the switch size for the SwGm mixer.

[1]Note: this assumption is not always accurate, especially not for small RTS-dominated MOSFET devices [13].

[2]In weak inversion, g_3 is positive, and the effect can be exploited te reduce nonlinearity.

TABLE II
OVERVIEW OF THE SIMULATION PARAMETERS USED FOR COMPARING THE SWITCHED TRANSCONDUCTOR AND CONVENTIONAL ACTIVE MIXER OF FIG. 4. NOTE THE DIFFERENCE IN SUPPLY VOLTAGE V_{dd}

Property	SwGm	Gm+Sw
W/L of Gm device	15/0.36	15/0.36
W/L of switch devices	15/0.18 (N), 30/0.18(P)	22.5/0.18 (N)
Common-mode LO-voltage switches	0.5V	1V
W/L of the LO-buffer	10/0.18 (N), 30/0.18 (P)	10/0.18 (N), 30/0.18 (P)
LO-signal driving the LO-buffer	0.5V bias, $0.5V_{pk}$ sine	0.5V bias, $0.5V_{pk}$ sine
Total R_L and load capacitance	2x2.5 Kohm and 2x1pF	2x2.5 Kohm and 2x1pF
Vdd, maximum gate voltage	1 Volt	1.5Volt

TABLE III
EFFECT OF THE WIDTH W_N AND W_P OF THE NMOS AND PMOS SWITCHES IN THE SWGM MIXER ON VARIOUS MIXER PROPERTIES, FOR AN IF FREQUENCY OF 10 MHz AND LO FREQUENCY OF 500 MHz (SEE TABLE II FOR OTHER PARAMETERS)

Remarks	W_N [μm]	W_P [μm]	CG [dB]	IIP3 [dBm]	ΔNF (dB)	$I_{D,on}$ (μA)	Pdis (mW)
Only Gm	no switch	no switch	-	9	-	228	-
	150	no switch	10.2	5	+1.7	213	0.8
	150	450	11.2	10	-1.0	212	1.6
	150	300	11.3	9	-1.3	213	1.4
	50	100	11.1	8	-1	200	0.82
final choice	***15***	***30***	***10.2***	***7***	***0***	***164***	***0.57***
	5	10	7.9	4	+0.5	107	0.4
split source	2 * 7.5	2 * 15	7.4	9	+0.9	163	0.6
sinewave LO	15	30	9.6	6	-0.2	164	0.4

A. Choice of Switches in the SwGm Mixer

Table III shows simulation results for the switched transconductor mixer for various choices of the switch transistor widths W_N and W_P. An LO frequency of 500 MHz was used to guarantee trapezium-like waveforms as assumed during the theoretical derivation. As expected from (14), the best linearity is achieved for wide switches: $\mathrm{IIP3} = 9$ dBm in that case, equal to the unswitched transconductance core.

The choice of the ratio W_P/W_N affects the ratio between the ON- and OFF-switching times and common-mode output currents. As PMOS transistors have mobility roughly three times lower, PMOS switches that are three times wider are optimal if the switches are very wide. If the PMOS is left out ($W_P = 0$), the transconductors switch on rapidly, but switch off slowly, injecting unwanted currents, leading to 1-dB gain reduction, 5-dB linearity penalty, and 2.7-dB worse NF. As the NMOS transconductor "helps" in switching off, the PMOS switch can be chosen smaller. For $W_P/W_N = 2$, the results are close to those for $W_P/W_N = 3$, indicating that the switch width is not very critical.

Simulations for decreasing switch width, keeping $W_P/W_N = 2$, results in a gradual degradation in conversion gain, linearity, and noise figure, while saving power. Accepting 1–2 dB degradation, the final choice used for comparison with the Gilbert mixer was $W_N = 15$ μm and $W_P = 30$ μm. Detailed analysis shows that the linearity coarsely follows (14), while the average drain bias voltage of the transconductor transistor also plays an important role (higher is better). A more detailed analysis as given in [14] is beyond the scope of this paper and is not straightforward as it requires a model for the nonlinearity of the drain–source conductance (e.g., [4]).

To avoid the nonlinearity due to source voltage variation, the switch transistors can be split in two, providing every transconductor transistor with a separate switch. This improves linearity but has the disadvantage that the conversion transconductance is reduced and that noise of the switch devices no longer is a common-mode output noise current (was not pursued further).

Last, but not least, we also simulated the SwGm mixer with a direct sinewave drive of the switches, without an additional LO buffer. The conversion gain and linearity is slightly degraded, but differences are smaller than 1 dB.

B. Comparing the SwGm and Gm+Sw Mixers

Let us now address the performance comparison of the two mixers. Table IV compares their performance, again at a 500-MHz LO frequency, but also at 2 and 6 GHz. Load resistors were chosen for a conversion gain of approximately 10 dB (see Table II). Fig. 6 shows the conversion gain versus LO frequency for both mixers. The difference in conversion gain is smaller

TABLE IV
SIMULATED MIXER PROPERTIES FOR THE MIXERS AS DEFINED IN TABLE II, FOR AN IF FREQUENCY OF 10 MHz AND LO FREQUENCIES OF 500 MHz, 2 GHz, AND 6 GHz. NOISE VOLTAGE VARIANCES ARE EVALUATED AT THE OUTPUT

	SwGm			Gm+Sw		
LO-frequency:	0.5GHz	2GHz	6GHz	0.5GHz	2GHz	6GHz
Conversion Gain [dB]	10.2	10.0	7.4	10.4	9.8	8.0
IIP3 [dBm]	7	6	5	10	7	6
NF (only thermal noise) [dB]	22.8	23.0	24.7	22.9	23.7	25.8
NF (also 1/f noise) [dB]	24.2	24.2	25.4	22.9	23.9	26.9
Gm, thermal noise [nV^2/Hz]	393	354	269	405	322	189
Gm, 1/f noise [nV^2/Hz]	173	136	58	<1	<1	<1
Sw, thermal noise [nV^2/Hz]	<1	<1	<1	23	98	265
Sw, 1/f noise [nV^2/Hz]	<1	<1	<1	2	24	148
Source R_s, thermal noise [nV^2/Hz]	5.0	4.4	2.4	5.3	4.3	2.7
Load R_L, thermal noise [nV^2/Hz]	77	78	79	80	74	62
P_{dis} LO-buffer [mW]	0.14	0.45	0.90	0.12	0.37	0.92
P_{dis} mixer [mW]	0.42	0.60	0.95	0.49	0.49	0.49

than 0.5 dB (due to the two cascaded LO buffer inverters in the switched transconductor case, the gain is slightly higher at a low LO frequency).

As expected from (14) and the Table III, at the 500-MHz LO frequency, the SwGm mixer has a 2-dB worse IIP3 then the (unswitched) transconductor. Provided that sufficient voltage headroom is available (a 1.5-V supply), the conventional mixer achieves even a 1-dB higher IIP3 then does the unswitched transconductor, most probably due to the cascode effect of the switches. However, at lower supply voltage, its linearity detoriates quickly (e.g., at $V_{\rm dd} = 1.25$ V we find 4 dBm). At higher LO frequencies, capacitive effects of the switch devices reduce linearity [14], and IIP3 values are very similar to that of the SwGm mixer.

Fig. 7 shows the output noise voltage as a function of LO frequency, at the 10-MHz IF frequency, where we can observe both thermal noise and $1/f$ noise effects, as they are almost equal. Clearly the two mixers in Fig. 7 show a very different trend: where the output noise of the SwGm mixer drops with the decrease in conversion gain at higher LO frequency, it increases for the conventional mixer. Table IV lists the variance of the output noise contributions in nV^2/Hz, allowing for a detailed comparison. Fig. 8 shows the resulting overall single sideband noise figure. As the $1/f$ noise of the conventional mixer is negligible at a low LO frequency, it has a 1.5-dB better noise figure there. However, at higher LO frequencies, the fundamental noise benefit of the SwGm mixer with respect to noise due to the switch devices becomes visible. Analysis for different conditions shows that 1–3-dB thermal noise benefit can be obtained. Furthermore, $1/f$ noise of the switch transistors also becomes more significant at a higher LO frequency in the conventional mixer (see $1/f$ noise data in Table IV). In this specific case, it even becomes worse than for the SwGm mixer at 6 GHz. In general, the SwGm has the nice property that the *noise goes down together with the useful signal*, while in the *conventional mixer the signal drops, and noise increases* due to the switch contribution.

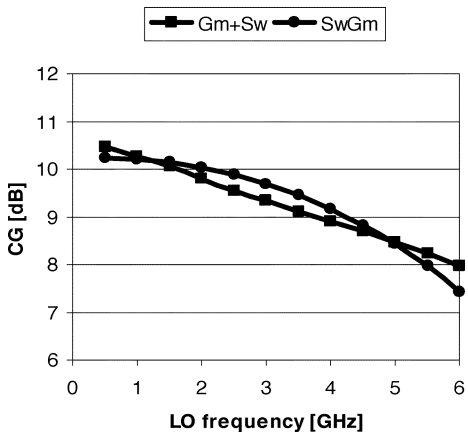

Fig. 6. Simulated conversion gain as a function of LO frequency for the SwGm and Gm+Sw mixers of Fig. 4.

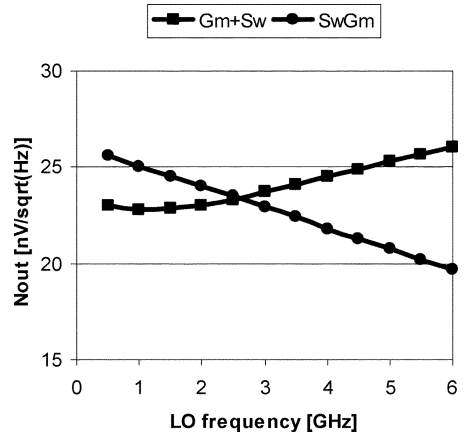

Fig. 7. Simulated output noise as a function of LO frequency for the SwGm and Gm+Sw mixers of Fig. 4. The different trend in noise is clearly visible.

The power consumption of the SwGm mixer consists of a static part for biasing the transconductance core (about 0.4 mW) and a dynamic part consumed in the LO driver. Overall, the current consumption in the SwGm mixer is slightly higher, due to the cascade of two inverters (LO buffer and mixer switches) in the SwGm mixer. Note that in many cases the switches of the SwGm mixer can be driven directly without an extra LO buffer, saving approximately half of the dynamic power consumption.

Overall, we conclude that the SwGm mixer renders competitive performance compared to a conventional active mixer at a 0.5-V lower $V_{\rm dd}$, reducing gate-oxide stress significantly.

VI. IC Implementation and Measurements

In order to verify the new mixer concept experimentally, a down-conversion mixer was designed to operate at a 1-V supply voltage. Fig. 9 shows the schematic, with a mixer core like Fig. 4(a) (M1–M6). Transistor sizes are close to those used in the simulations in the previous section. However, the mixer switches are directly driven by antiphase sine-wave signals balanced around a common-mode voltage, equal to the switch point of the inverters. Note that full-swing digital signals can also be used and actually give slightly higher conversion gain and linearity in simulation (see Table III).

To generate an output voltage, an I–V converter must be added. To allow for variable gain to adapt to different input signals and to allow for experimental freedom, the mixer was designed for a maximum conversion gain of around 20 dB ($R_{o1} = R_{o2} = 10$ kohm), which can be lowered by adding a single external resistor between the output V_{o1} and V_{o2}. In the measurements that follow, an external resistor was chosen to achieve 12 dB of conversion gain. The common-mode current of the mixer is absorbed by two PMOS transistors in the upper part of Fig. 9, allowing for more conversion gain (but at the cost of additional output noise). Bias current source I_b shifts the common-mode output voltage up to a value around 0.6 V, to fit in the 1-V supply voltage.

The mixer was fabricated in a standard industrial 0.18-μm CMOS process. Fig. 10 shows a photograph of the mixer core. Termination resistors of 50 Ω were added on chip for all of the RF and LO inputs for ease of measurement. The chip was measured via wafer probing, using baluns for single to differential conversion at the input. A differential probe was used to measure the differential output voltage. The IF bandwidth was limited to 2 MHz, mainly due to the input capacitance of the differential probe. The conversion gain as a function of LO frequency was measured using two baluns with overlap in frequency range: one for the 300-MHz–3-GHz band and one for 2–18 GHz. The measurements are shown in Fig. 11. Despite the experimental inaccuracies, it can be concluded that the mixer has the expected 12-dB conversion gain and a -3-dB LO bandwidth of approximately 4 GHz, which is in reasonable agreement with simulation. The current consumption of the mixer consists of a more or less constant term of 180 μA for the transconductors core, and a dynamic term determined by the switching (≈ 200 μA/GHz). Note that the power consumption is low because the transconductance is rather low, resulting in a high equivalent input noise resistance. To achieve better than a 15-dB noise figure with respect to

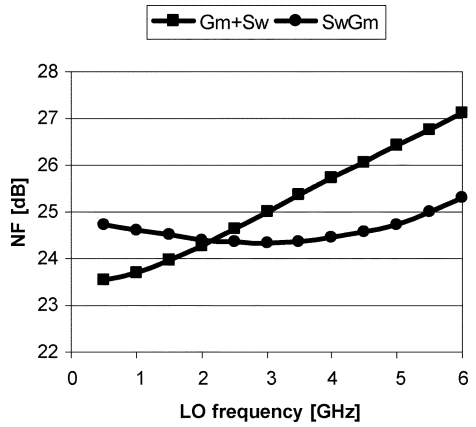

Fig. 8. Simulated single sideband noise figure with respect to 50 Ω as a function of the LO frequency for the SwGm and Gm+Sw mixers of Fig. 4.

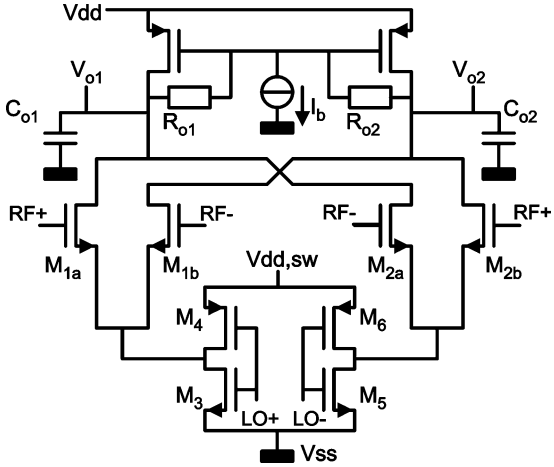

Fig. 9. Double-balanced switched transconductor mixer implemented on chip.

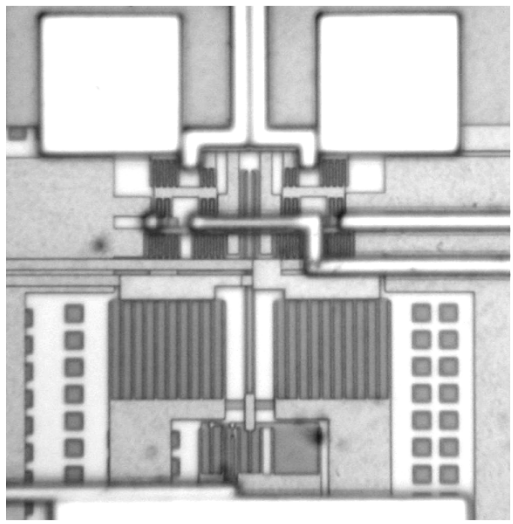

Fig. 10. Chip photograph of the switched transconductor mixer core (0.18-μm CMOS, 75 μm $\times$ 65 μm).

50 Ω, a transconductance roughly 10 times higher is needed. By means of admittance level scaling [12], this can easily be achieved without affecting bandwidth and linearity, by scaling up all W values by a factor of 10, at the cost of 10 times power consumption. At 1 GHz, this will result in approximately $10 \times (0.18 + 0.2)$mW $\cong 4$ mW total power consumption.

Fig. 12 shows the linearity of the mixer as a function of frequency. An IIP3 better than +4 dBm is typically achieved for 12-dB conversion gain. Simulations and experiments with varying R_o showed that this linearity is limited by the nonlinearity of the output conductance. Actually, conversion gain and IIP3 can be traded, where 1 dB more of conversion gain renders 1 dBm less IIP3.

The remarkable noise properties of the new mixer were also verified by measurements. Fig. 13 shows the measured output noise voltage as a function of the LO frequency, measured at 1-MHz IF frequency. The $1/f$ corner frequency was found to be around 1 MHz, considerably lower than the 10 MHz found in simulations (simulation parameters model worst case $1/f$ noise). Thus, a mix of $1/f$ noise and thermal noise determines the output noise, more or less as in the simulations in the previous section. Even though the PMOS transistor in the I–V converter increase the output noise compared to Fig. 7, the noise clearly decreases with increasing LO frequency, as predicted based on the noise analysis in Section IV.

VII. Conclusion

A CMOS switched transconductor mixer has been presented, which can operate at a 1-V supply voltage in a 0.18-μm CMOS technology with threshold voltages of 0.5 V. It requires almost no voltage headroom across the switch and does not require gate-drive voltages outside the supply rails, because only switches with a conductive channel connected to either $V_{\rm ss}$ or $V_{\rm dd}$ are used. As a result, the gate-oxide stress of the switch devices is low, as desired for reliability reasons. By using low ohmic switches with a low-voltage drop compared to $V_{\rm dd}$, almost the full supply voltage headroom can be reserved for the transconductance device and load, allowing for more conversion gain. The LO port of the mixer can be driven dc-coupled with full-swing CMOS signals with a noncritical common-mode voltage. The mixer basically realizes the same transfer function as a conventional active mixer, but instead of switching currents after V–Iconversion, two transconductors with cross-coupled outputs are alternatingly switched on and off. In contrast to conventional active and passive CMOS mixers, the noise produced by the switch transistors is common-mode noise, which is rejected at the differential output. As a result, when the LO frequency goes up, the output noise goes down together with the useful output signal, while in the conventional mixer the signal drops, and noise increases due to the switch contribution. As a consequence, a 1–3-dB lower noise figure can be achieved at high LO frequencies, where the noise contribution of the switch transistors becomes significant in conventional mixers. Overall, similar mixer performance is achieved, but at a significantly lower supply voltage directly compatible with current and future CMOS processes.

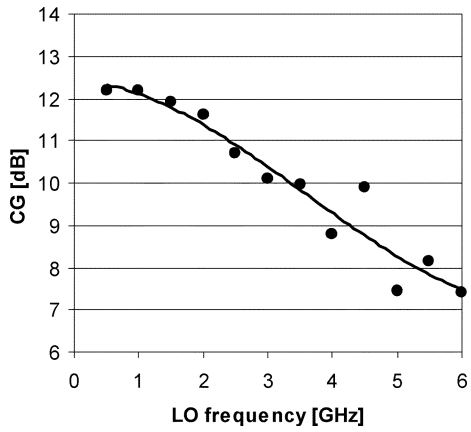

Fig. 11. Measured conversion gain as a function of the LO frequency.

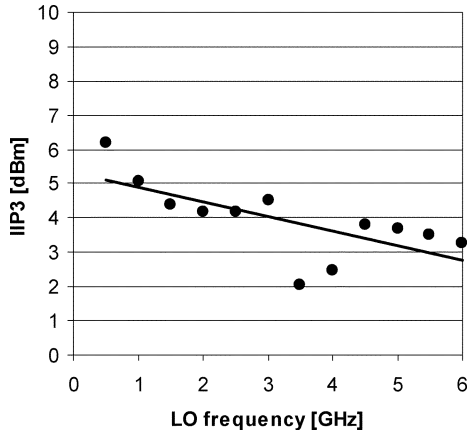

Fig. 12. Measured IIP3 as a function of the LO frequency.

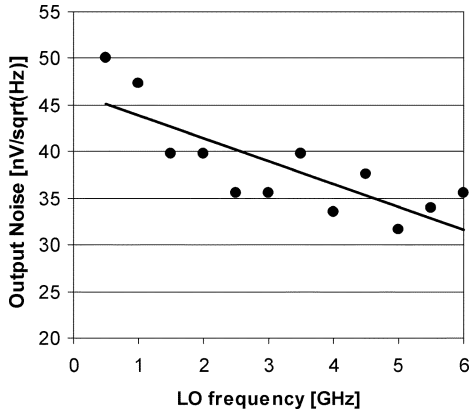

Fig. 13. Measured output noise voltage at a 1-MHz IF frequency versus the LO frequency.

Acknowledgment

The authors would like to thank the reviewers for very useful suggestions. The authors would also like to acknowledge Philips Research Laboratories for the IC implementation and E. Stikvoort, J. Vergara, V. Arkesteijn, and H. de Vries for useful discussions.

REFERENCES

[1] T. Lee, *The Design of CMOS Radio-Frequency Circuits*. Cambridge, U.K.: Cambridge Univ. Press, 1998.

[2] J. Crols and M. Steyaert, "Switched opamp: an approach to realize full CMOS switched-capacitor circuits at very low power supply voltages," *IEEE J. Solid-State Circuits*, vol. 29, pp. 936–942, Aug. 1994.

[3] E. A. M. Klumperink, S. M. Louwsma, G. J. M. Wienk, and B. Nauta, "A 1 Volt switched transconductor mixer in 0.18 μm CMOS," in *Proc. 2003 Symp. VLSI Circuits*, Kyoto, Japan, June 2003, paper 17-3, JSAP ISBN 4-89114-035-6 (4 pages, CD-ROM).

[4] R. van Langevelde and F. M. Klaassen, "Accurate drain conductance modeling for distortion analysis in MOSFETs," in *IEDM Tech. Dig.*, 1997, pp. 313–316.

[5] S. Kang, B. Choi, and B. Kim, "Linearity analysis of CMOS for RF application," in *IEEE MTT-S Int. Microwave Symp. Dig.*, 2002, pp. 279–282.

[6] M. Tiebout and T. Liebermann, "A 1 V fully integrated CMOS transformer based mixer with 5.5 dB gain, 14.5 dB SSB noise figure and 0 dBm input IP3," in *Proc. 29th Eur. Solid-State Circuits Conf.*, 2003, pp. 73–76.

[7] Q. Li, W. Li, J. Zhang, and J. S. Yuan, "Soft breakdown and hot carrier reliability of CMOS RF mixer and redesign," in *IEEE MTT-S Int. Microwave Symp. Dig.*, 2002, pp. 509–512.

[8] H. Iwai, "CMOS technology—year 2010 and beyond," *IEEE J. Solid-State Circuits*, vol. 34, pp. 357–366, Mar. 1999.

[9] M. S. J. Steyaert, J. Janssens, B. De Muer, M. Borremans, and N. Itoh, "A 2-V CMOS cellular transceiver front-end," *IEEE J. Solid-State Circuits*, vol. 35, pp. 1895–1907, Dec. 2000.

[10] M. T. Terrovitis and R. G. Meyer, "Noise in current-commutating CMOS mixers," *IEEE J. Solid-State Circuits*, vol. 34, pp. 772–783, June 1999.

[11] H. Darabi and A. A. Abidi, "Noise in RF-CMOS mixers: A simple physical model," *IEEE J. Solid-State Circuits*, vol. 35, pp. 15–25, Jan. 2000.

[12] E. A. M. Klumperink and B. Nauta, "Systematic comparison of HF CMOS transconductors," *IEEE Trans. Circuits Syst. II*, vol. 50, pp. 728–741, Oct. 2003.

[13] A. P. v. d. Wel, E. A. M. Klumperink, L. K. J. Vandamme, and B. Nauta, "Modeling random telegraph noise under switched bias conditions using cyclostationary RTS noise," *IEEE Trans. Electron Devices*, vol. 50, pp. 1378–1384, May 2003.

[14] M. T. Terrovitis and R. G. Meyer, "Intermodulation distortion in current-commutating CMOS mixers," *IEEE J. Solid-State Circuits*, vol. 35, pp. 1461–1473, Oct. 2000.

Eric A. M. Klumperink (M'98) was born on April 4, 1960, in Lichtenvoorde, The Netherlands. He received the B.Sc. degree from HTS, Enschede, The Netherlands, in 1982. After a short period in industry, he joined the Faculty of Electrical Engineering of the University of Twente in 1984, where he was mainly engaged in analog CMOS circuit design. This resulted in several publications and a Ph.D. thesis, in 1997, on the subject of transconductance-based CMOS circuits.

He is currently an Assistant Professor in the IC Design group, which participates in the MESA+ Research Institute. He holds four patents and has authored or coauthored more than 50 journal and conference papers. His research interest is in design issues of HF CMOS circuits, especially for front-ends of integrated CMOS transceivers.

Dr. Klumperink is a corecipient of the ISSCC 2002 Van Vessem Outstanding Paper Award.

Simon M. Louwsma was born on January 1, 1976, in Wommels, The Netherlands. In 2001, he received the M.Sc. degree in electrical engineering from the University of Twente, Enschede, The Netherlands. Since 2001, he has been working toward the Ph.D. degree in the IC Design group of the MESA+ Research Institute and the Department of Electrical Engineering at the same university.

His research interests include high speed A/D converters and other analog and mixed signal circuits and systems in CMOS.

Gerard J. M. Wienk was born on October 11, 1958, in Hengelo, The Netherlands. From 1982 to 2001, he was with different companies working in the field of computer hardware and operating systems. In 1992, he received the B.Sc. degree in electrical engineering from the Hogeschool Enschede, The Netherlands.

In July 2001, he joined the IC Design group of the MESA+ Research Institute, University of Twente, Enschede, The Netherlands, as a CAD Support Engineer. As well as supporting the IC design software environment, he is also involved in the realization process of designs and measurement of prototype ICs.

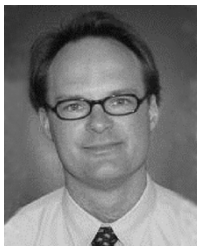

Bram Nauta (M'91–SM'03) was born in Hengelo, The Netherlands, in 1964. In 1987, he received the M.Sc degree (*cum laude*) in electrical engineering from the University of Twente, Enschede, The Netherlands. In 1991, he received the Ph.D. degree from the same university on the subject of analog CMOS filters for very high frequencies.

In 1991, he joined the Mixed-Signal Circuits and Systems Department of Philips Research, Eindhoven, The Netherlands, where he worked on high-speed A/D converters. From 1994, he led a research group in the same department, working on analog key modules. In 1998, he returned to the University of Twente as full Professor heading the IC Design group of the MESA+ Research Institute and the Department of Electrical Engineering. His current research interest is analog CMOS circuits for transceivers. He is also a part-time consultant in industry, and in 2001, he cofounded Chip Design Works. His Ph.D. thesis was published as the book *Analog CMOS Filters for Very High Frequencies* (Kluwer, 1993). He holds 10 patents in circuit design.

Dr. Nauta received the Shell Study Tour Award for his Ph.D. work, and he is a corecipient of the ISSCC 2002 Van Vessem Outstanding Paper Award. From 1997 to 1999, he served as Associate Editor of IEEE TRANSACTIONS ON CIRCUITS AND SYSTEMS, PART II—ANALOG AND DIGITAL SIGNAL PROCESSING, and in 1998 he served as Guest Editor for IEEE JOURNAL OF SOLID-STATE CIRCUITS. In 2001, he became an Associate Editor for IEEE JOURNAL OF SOLID-STATE CIRCUITS. He is a member of the technical program committee of ESSCIRC and ISSCC.